Studying radiative charm meson decays at the LHCb experiment

Aleksei Chernov

IFJ PAN

July 11, 2022

Place of charm physics within the Standard Model

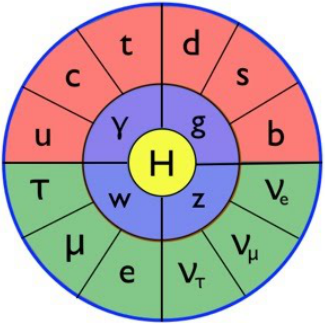

$V_{ud} \approx 1 - \lambda^2$	$V_{us} \approx \lambda$	$V_{ub} \approx A\lambda^3(\rho - i\eta)$
$V_{cd} \approx -\lambda$	$V_{cs} \approx 1 - \lambda^2$	$V_{cb} \approx A\lambda^2$
$V_{td} \approx A\lambda^3(1 - \rho - i\eta)$	$V_{ts} \approx -A\lambda^2$	$V_{tb} = 1 + O(\lambda^3)$

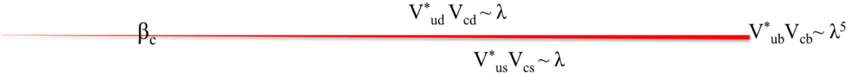

Status of CP violation in charm

- Small in the Standard Model, as illustrated by Charm's UT (above)
- First discovery - LHCb in early 2019, using combined Run 1 and Run 2 data of $D^0 \to hh$ decays, $> 5\sigma$ observation of $\Delta A_{CP} = A_{CP}(KK) - A_{CP}(\pi\pi) = (-15.4 \pm 2.9) \times 10^{-4}$
- All measurements of the invidivual asymmetries of $D^0 \to hh$ are consistent with zero so far.

Radiative charm decays

Object of our study is prompt $\boldsymbol{D*^{+} \to (D^{0} \to V\gamma)\pi^{+}}$(c.c implied) decays, where $\boldsymbol{V}$ stands for a vector meson - $\boldsymbol{\rho, \phi}$ or $\boldsymbol{K^{*}}$

- Flavour changing neutral current - suppressed by GIM mechanism in the Standard Model.
- Significant asymmetries allowed in the SM, possibly further enhanced by BSM particles entering the penguin .

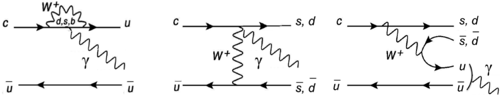

Figure 2: Examples of short-distant radiative penguin decay $\boldsymbol{D^{0}} \to \rho\gamma$, radiative $\boldsymbol{W}$ exchange and possible long distance effect (right).

Nuisance asymmetries

The raw asymmetry is measured in a simple counting experiment:

$$A_{raw} = \frac{N(D^0) - N(\bar{D}^0)}{N(D^0) + N(\bar{D}^0)}$$

This observable asymmetry can be split into three different categories: physical CP asymmetry, production asymmetry - more $\bar{D}^0$ produced in pp collisions than D^0, and detection asymmetry associated with each charged particle (LHCb detector is made out of ordinary matter, and interaction cross-sections for h^+ and h^- differ):

$$A_{raw} = A_{CP} + A_{prod.} + A_{det.}(hh) + A_{det}(\pi_s)$$

This necessiates the use of normalisation channels to get rid of nuisance asymmetries.

Analysis strategy

- We analyze data collected by the LHCb detector during the Run 1 and Run 2 (treated separately) with a trigger requiring two charged tracks and a photon-like calorimeter cluster that can be reconstructed as D^0, plus a 'slow' (low p^T) charged pion to identify the flavour.
- Main background is $D^0 \to hh\pi^0$ processes where the final $\pi^0 \to \gamma\gamma$ cluster is falsely identified as a single photon; in the low invariant mass regions significant contribution of $\eta \to \gamma\gamma$ is observed.
- We perform a multi-dimensional fit to three observables:
  - invariant mass $M(D^0)$
  - cosine of the helicity angle of the final state charged hadron $cos(\theta)$ - vital to distinguish between the radiative signal and π^0 peaking background. $V\gamma$ signal has the shape $(1 - cos^2(\theta)) \times acceptance$, peaking around $\cos(\theta) = 0$
  - Mass difference $\Delta M = M(D^{*+}) - M(D^0)$ - needed to take into account the5 combination of a good D^0 meson with a random slow pion - this type of combinatorial background produces a peak in M, but is flat in ΔM. Mistagged D^0's ***can affect asymmetry***.

2D fit to the $K^*\gamma$ calibration subsample ($cos(\theta) < -0.7$)

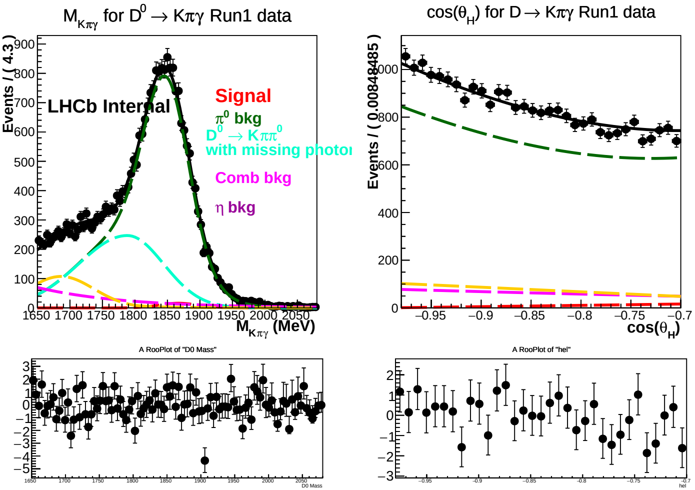

Figure 3: Helicity edge - where we expect no or negligible signal - is used to calibrate parameters of the PDFs in order to lessen reliance on MC.

Fit projections - $M(D^0)$ in bins of $cos(\theta)$

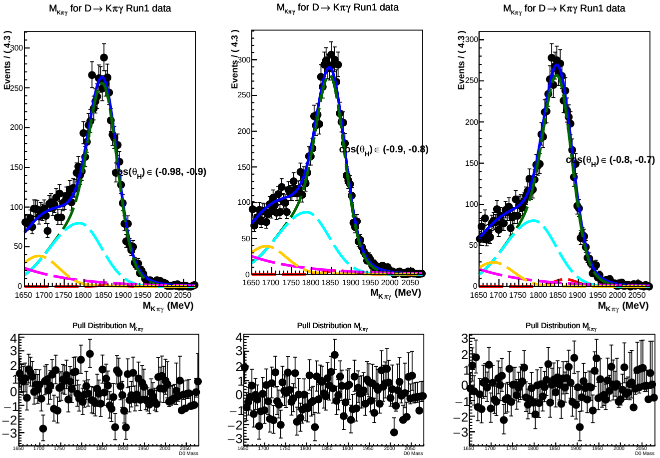

Figure 4: We expect $\cos(\theta)$ and $M(D^0)$ to be independent observables and this assumption seems to hold.

Fit projections - $cos(\theta)$ in bins of $M(D^0)$

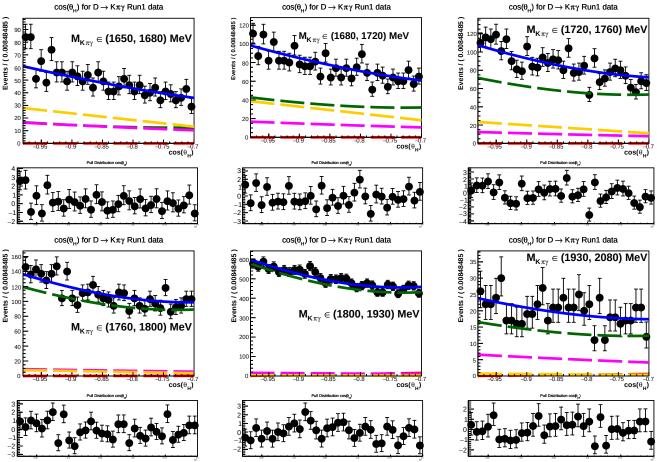

Figure 5: We expect $\cos(\theta)$ and $M(D^0)$ to be independent observables and this assumption seems to hold.

2D fit to the $K^*\gamma$ sample in the signal helicity region

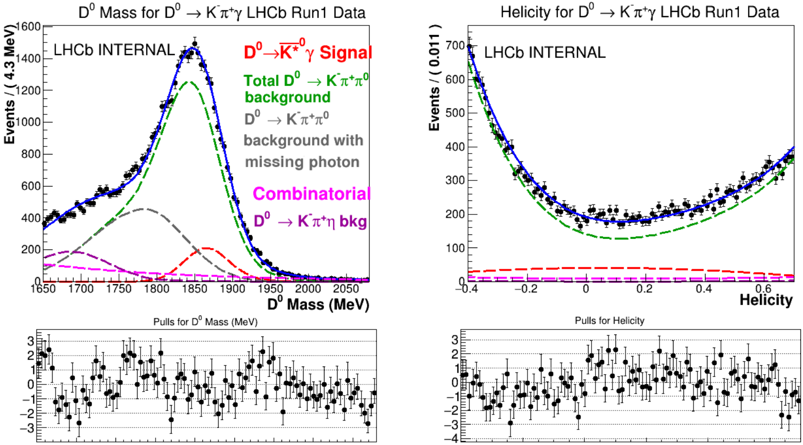

Figure 6: Preliminary fit to the $D^0 \to K^*\gamma$ sample. After splitting by the charge of tagging pion, from a similar simultaneous fit we can extract A_{raw}.

Fit projections - invariant D^0 mass in bins of helicity

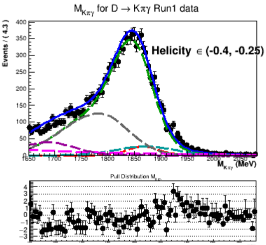

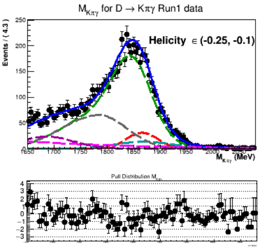

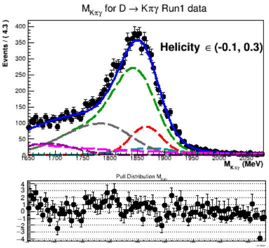

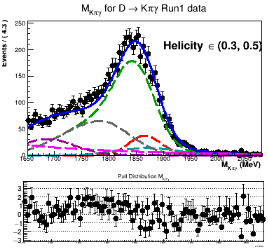

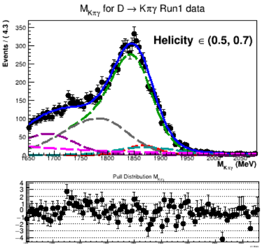

Fit projections - cos(θ) in bins of invariant mass

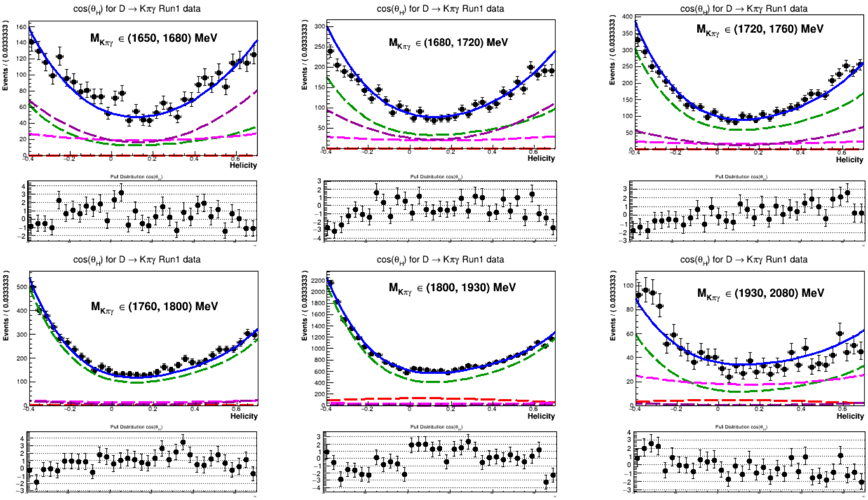

Shape of the ΔM component from the $K^*\gamma MC$ for 2012 run conditions

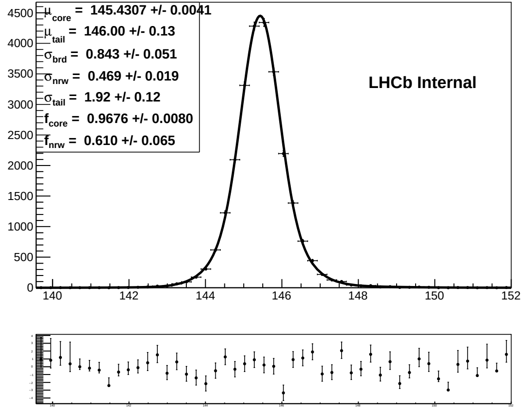

Figure 7: Shape used - double Gaussian with a common mean. A third, very wide Gaussian is added with a small ($< 4\%$) fraction to take care of the outliers.

Data-MC difference - calibration and correlations

- Calibration sample is selected along the edges of the helicity angle, where the signal is small or negligible. The purpose of this fit is to take possible data-MC difference into account. We assume that helicity angle θ is not correlated with either D^0 invariant mass or ΔM.
- For the other two variables, such an assumption does not hold up - resolution of ΔM peak depends on the mass (or vice versa).
- The simplest possible solution to this problem we've found is to introduce a scale factor to the ΔM resolution that depends on the $M(D^0)$:

$$\sigma_{\Delta M}(M(D^0)) = \sigma_{MC} \times \lambda \,|\, \lambda = P^N(M(D^0))$$

ΔM fits in bins of mass

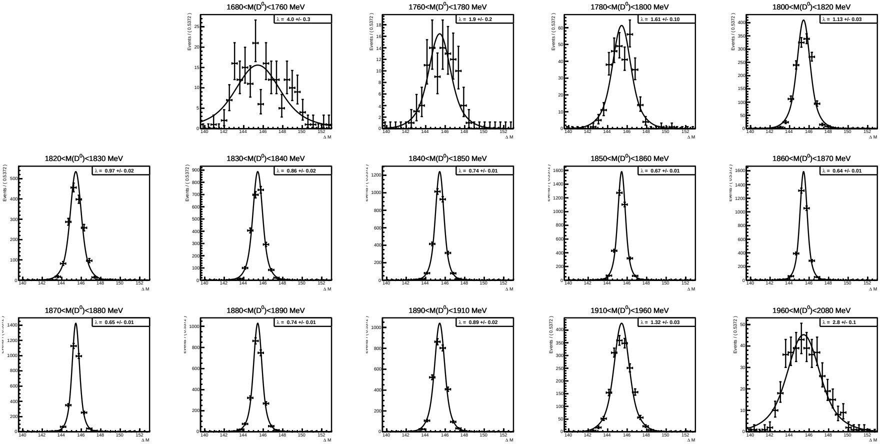

Figure 8: Fits in mass bins using the fixed shape from slide 13 multiplied by a scale factor λ - get an estimation of $\sigma_{\Delta M}(M(D^0))$.

Parametrizing $\lambda(M)$ curve

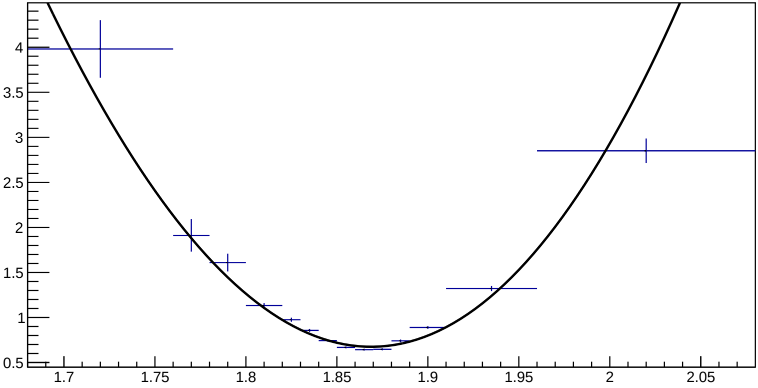

Figure 9: Fit to the $\lambda(M)$ taken from the slide above; function used is P^3.

Thank you for your attention!